SELF-SIMILAR MOTIONS OF A GAS WITH SHOCK WAVES, SPREADING ACCORDING TO A POWER LAW INTO A GAS AT REST

(AVTOMODEL'NYE DVIZHENIIA GAZA S UDARNYMI VONAMI, RASPROSTRANIAIUSHCHIMISIA PO STEPENNOMU ZAKONU PO POKOIASHCHEMUSIA GAZU)

PMM Vol.23, No.5, 1959, pp. 936-939

G.L. GRODZOVSKII and N.L. KRASHCHENNIKOVA
(Moscow)

(Received 22 May 1959)

As is well known, the problem of uniform unsteady motion of a gas reduces to the problem of integration of a set of partial differential equations. Sedov has shown [1] that for problems determined by only two dimensionally independent parameters, besides the radial distance r and time t, the partial differential equations can be replaced by ordinary differential equations, corresponding to the self-similar motions of the gas.

One example of such self-similar motions occurs when a "piston" located at r expands according to the law $r = Ct^m$ in a gas with an initial density ρ_1 and an initial pressure $p_1 = 0$ (which corresponds to an infinitely large pressure jump across the shock wave generated by the motion of the piston).

Solutions for such motions were carried out in references [2,3,4]. Reference [5] has established that self-similar motion takes place only for a limited range of the exponent m, namely for $m > 2/(2 + \nu)$ where $\nu = 1, 2, 3$ correspond to the plane, cylindrically, and spherically symmetric problems, respectively. The present paper treats a more general case of self-similar motions.

Consider self-similar motions of gas with shock waves which spread into quiescent gas according to the power law

$$D = Ct^n \qquad (\rho_1 = \text{const}, \qquad p_1 = 0) \tag{1}$$

where D is the shock velocity.

This class of motions includes both diverging and converging flows. One example of converging flows is that of a strong peripheral shock wave [6]:

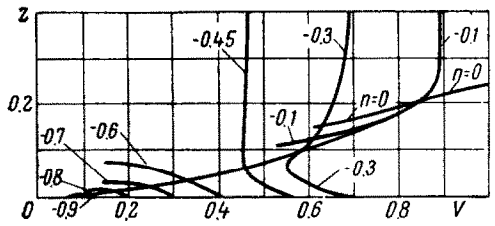

Fig. 1.

$$D \sim t^{\frac{-\nu}{2+\nu}} \qquad \text{for } t < 0 \qquad (2)$$

One can form only one dimensionless combination

$$\lambda = \frac{Ct^{n+1}}{r} \qquad (3)$$

out of the parameters which determine the problem. When use is made of the dimensionless functions defined by the relations

$$v = \frac{r}{t} V(\lambda), \quad \rho = \rho_1 R(\lambda), \quad p = \frac{\rho_1 r^2}{t^2} P(\lambda), \quad z = \frac{\varkappa P}{R} \qquad (4)$$

the following set of equations is obtained [2]: (5)

$$\frac{dz}{dV} = z\frac{[2(V-1)+\nu(\varkappa-1)V](V-n-1)^2-(\varkappa-1)V(V-1)(V-n-1)-[2(V-1)-2n(\varkappa-1)/\varkappa]z}{(V-n-1)[V(V-1)(V-n-1)-(2n/\varkappa+\nu V)z]}$$

$$\frac{d\ln\lambda}{dV} = \frac{(V-n-1)^2-z}{V(V-1)(V-n-1)-(2n/\varkappa+\nu V)z} \qquad (6)$$

$$\frac{d\ln R}{d\ln\lambda}(V-n-1) = \frac{V(V-1)(V-n-1)-(2n/\varkappa+\nu V)z}{z-(V-n-1)^2} + \nu V \qquad (7)$$

The solution of the problem is found by integrating the system (5) - (7) with the given initial conditions:

$$p_2 = \frac{2}{\varkappa+1}\rho_1 D^2 = \frac{2}{\varkappa+1}\rho_1 C^2 t^{2n}, \quad v_2 = \frac{2}{\varkappa+1}D = \frac{2}{\varkappa+1}Ct^n, \quad \rho_2 = \frac{\varkappa+1}{\varkappa-1}\rho_1 \qquad (8)$$

$$r_2 = \int D dt = \frac{1}{n+1}Ct^{n+1}, \quad \lambda_2 = \frac{Ct^{n+1}}{r_2} = n+1, \quad V_2 = \frac{v_2}{r_2}t = 2\frac{n+1}{\varkappa+1} \qquad (9)$$

$$R_2 = \frac{\rho_2}{\rho_1} = \frac{\varkappa+1}{\varkappa-1}, \quad P_2 = \frac{p_2 t^2}{\rho_1 r_2^2} = \frac{2}{\varkappa+1}(n+1)^2, \quad z_2 = \frac{\varkappa P_2}{R_2} = \frac{2\varkappa(\varkappa-1)}{(\varkappa+1)^2}(n+1)^2$$

$$\text{at piston } V_1 = n+1 \qquad (10)$$

Figure 1 displays the integral curves in the V, z plane for $\nu = 2$ and $-1 \leqslant n \leqslant 0$. The calculations were carried out on the electronic computer "Strela" (Arrow). The solutions are found on both sides of the locus (V_2, z_2) of the conditions just behind the shock: diverging flows correspond to the upper branches of the curves and converging flows to the lower branches. The diverging flows for $n > -0.5$ correspond to the outward piston motion according to the power law. For $n = -0.5$ one has the blast wave solution either at the center or on the periphery. The rest of the flows are bounded in the V, z plane by a curve on which the parameter λ takes on extremal values. The pressure, density, and velocity fields are displayed in Figs. 2, 3 and 4. Here curves to the right correspond to

converging flows and curves to the left to diverging flows.

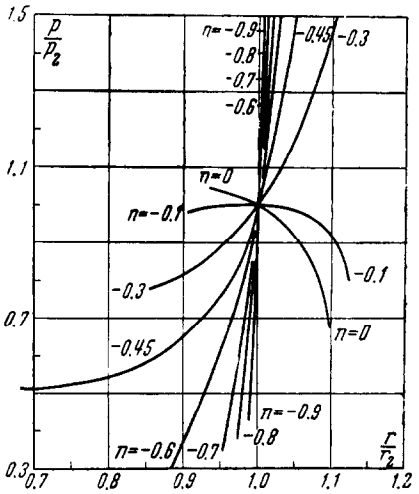

Fig. 2.

Let us consider some applications of these results. According to the law of hypersonic similarity and Mach number idependence of the drag coefficient [7] for geometrically similar bodies, the product of the wave-drag coefficient and the square of the fineness ratio is a constant (independent of M)

$$C_x L^2 = C^* = \text{const} \tag{11}$$

The value of C^* can be determined conveniently from the solution of the flow around the thin body as M approaches infinity, where the well-known analogy with turbulent flow is helpful. The results in Figs. 2-4 facilitate the evaluation of wave-drag coefficients of axisymmetric bodies for which the shock shape follows a power law*.

The dimensionless pressure behind the shock wave as $M \to \infty$ becomes

$$p^0 = \frac{p - p_\infty}{1/2 \rho_\infty v_\infty^2} = \frac{4}{\varkappa + 1} \varepsilon^2 \tag{12}$$

Here ϵ is the local shock angle which is related to the local body slope**

---

* Detailed theoretical and experimental results for such bodies in English can be found in T. Kubota's *Investigation of Flow Around Simple Bodies in Hypersonic Flow*, GALCIT, Hypersonic Res. Project, Memo No. 40, June 1957.

** Presumably ω.

$$\frac{\omega}{\varepsilon} = \frac{r_0}{r_2} = r_{20} \tag{13}$$

where r_0 is the body radius. The local pressure coefficient at the body is

$$p_i^0 = \frac{4}{\varkappa + 1} \frac{\omega^2 p_{20}}{r_{20}^2} \tag{14}$$

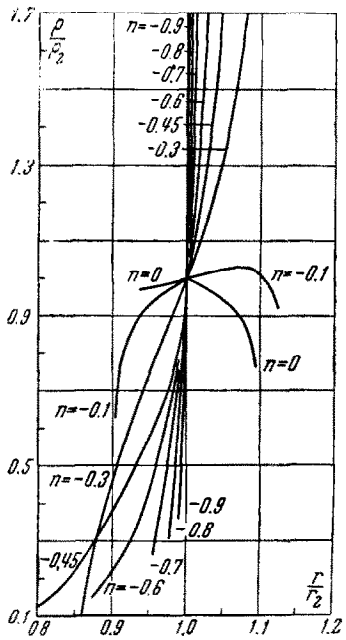

Fig. 3.

Consequently, the wave-drag coefficient is obtainable from the expression

$$C_x = \int_{r_*}^{1} p_i^0 d(r^2) = \frac{8}{\varkappa + 1} \frac{p_{20}(n+1)^2}{r_{20}^2 L^2} \int_{r_*}^{1} r^\mu dr$$

$$\left(\mu = \frac{3n+2}{n+1}\right)$$

Here L represents the fineness ratio, body length to maximum body radius. Unsteady axisymmetric diverging flows with $-0.5 < n < 0$ in Figs. 1-4 correspond to steady flows around axisymmetric bodies for which r_0 follows a power law. The values of p_{20}, r_{20} and $C_a L^2$ for these cases are given in the Table.

These results show that for hypersonic speeds with adiabatic exponent $\kappa = 1.4$ the smallest drag of bodies obeying a power-law is attained for $r_0 = Cx^{0.70}$. Therefore, the optimal axisymmetric shape of a body for very large Mach numbers will be fuller than that indicated for Newtonian pressure law, namely $r_0 = Cx^{0.75}$. The drag of this optimal shape is 27 per cent less than that of the cone with equal fineness ratio.

The variation of the wave-drag coefficient C_x of bodies obeying a power-law with volume Q is shown in Fig. 5, where the primes indicate properties of the circular cone.

In Fig. 6 curve 1 represents* the solutions for flows around circular cones obtained by the present method, to be compared with the circles computed by the usual integration of conical flows for $M = 10.94$. Curve 2 corresponds to flows around bodies with $r_0 = Cx^{0.7}$.

---

* Note change in notation: here L is true length, rather than the fineness ratio.

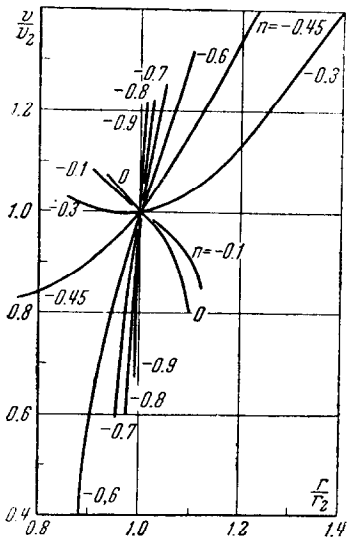

Fig. 4.

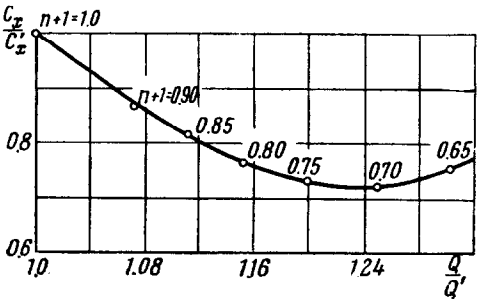

Fig. 5.

The example covers the practical optimization of body nose shapes in hypersonic flight as far as the wave drag is concerned. It is worth noting also the distribution of densities and pressures at the body which effect the heat transfer favorably.

TABLE

n	0	−0.1	−0.15	−0.2	−0.25	−0.3	−0.35	−0.4	−0.45
p_{20}	1.0497	0.983	0.942	0.891	0.836	0.78	0.713	0.6177	0.5121
r_{20}	0.9149	0.9053	0.8977	0.8888	0.8751	0.8567	0.8293	0.7771	0.6648
$C_x L^2$	2.091	1.822	1.71	1.604	1.533	1.517	1.583	1.8411	3.213

Similarly, other parametric regions in Figs. 2-4 can be utilized to predict flows for which shocks follow a power law. Thus axisymmetric diverging flows for $n < -0.5$ correspond to exterior flows around open bodies which allow through-flow. Turbulent converging flows can be utilized for evaluation of corresponding internal axisymmetric steady flows. As an example, curve *1* in Fig. 7 represents the internal body contour and curve 2 the shock wave corresponding to the shock shape $x = kr^2$. It must be noted that in these flows the entropy changes take place only inside the shock wave and that downstream from it the compression is isentropic along streamlines (see pressure variations in Fig. 2).

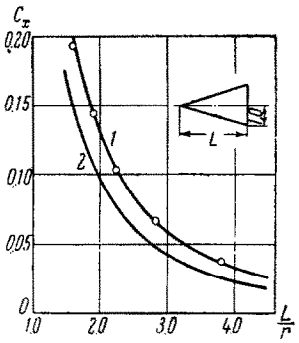

Fig. 6.

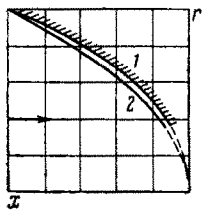

Fig. 7.

The authors express their appreciation to V.A. Cheprasov for his help with calculations.

BIBLIOGRAPHY

1. Sedov, L.T., *Metody podobia i razmernosti v mekhanike (Methods of Similarity and Dimensional Analysis in Mechanics)*. Izd. 4, GITTL, 1957.

2. Krashchennikova, N.L., O neustanovivshemsia dvizhenii gaza, vytiesniaemogo porshniem (On the unsteady motion of gas compressed by a piston). *Izv. Akad. Nauk SSSR, O.T.N.* No. 8, 1955.

3. Grodzovskii, G.L., Nekotorye osobennosti obtekania tiel pri bolshikh sverkhzvukovykh skorostiakh (Some properties of hypersonic flows around bodies). *Izv. Akad. Nauk SSSR, O.T.N.* No. 6, 1957.

4. Grodzovskii, G.L., Polieznaia interferentsia kryla i fiuzelazha pri giperzvukovykh skorostiakh (Favorable interference between wing and fuselage at hypersonic speeds). *Izv. Akad. Nauk SSSR, O.T.N.* No. 1, 1959.

5. Grigorian, S.S., Zadacha Koshi i zadacha o porshnie dlia odnomernykh neustanovivshikhsia dvizhenii gaza (avtomodelnye dvizhenia) (The problem of Cauchy and the problem of piston motion in the uniform unsteady flow of gas - self-similar motion). *PMM* Vol. 22, No. 2, 1958.

6. Grodzovskii, G.L., Avtomodelnoe dvizhenie gaza pri silnom pereferiinom vzryve (Self-similar motion of gas for a strong peripheral shock wave). *Dokl. Akad. Nauk SSSR*, Vol. 3, No. 5, 1956.

7. Tsien, H.S., Similarity laws of hypersonic flows. *J. Math. Phys.* Vol. 25, No. 3, 1946.

Translated by M.V.M.